Design of oscillatory dynamics in numerical simulations of compartment-based enzyme systems

Anna S. Leathard ; Paul A. Beales ; Annette F. Taylor ✉

Check for updates

View Online   Export Citation   CrossMark

Design of oscillatory dynamics in numerical simulations of compartment-based enzyme systems

View Online　　　Export Citation　　　CrossMark

Anna S. Leathard,[1] [ID] Paul A. Beales,[2] [ID] and Annette F. Taylor[1,a] [ID]

AFFILIATIONS

[1] Department of Chemical and Biological Engineering, University of Sheffield, Sheffield S1 3JD, United Kingdom
[2] School of Chemistry and Astbury Centre for Structural Molecular Biology, University of Leeds, Leeds LS2 9JT, United Kingdom

[a] Author to whom correspondence should be addressed: a.f.taylor@sheffield.ac.uk

ABSTRACT

Enzymatic reactions that yield non-neutral products are known to involve feedback due to the bell-shaped pH-rate curve of the enzyme. Compartmentalizing the reaction has been shown to lead to transport-driven oscillations in theory; however, there have been few reproducible experimental examples. Our objective was to determine how the conditions could be optimized to achieve pH oscillations. We employed numerical simulations to investigate the hydrolysis of ethyl acetate in a confined esterase enzyme system, examining the influence of key factors on its behavior. Specific parameter ranges that lead to bistability and self-sustained pH oscillations and the importance of fast base transport for oscillations in this acid-producing system are highlighted. Suggestions are made to expand the parameter space for the occurrence of oscillations, including modifying the maximum of the enzyme pH-rate curve and increasing the negative feedback rate. This research not only sheds light on the programmable nature of enzyme-driven pH regulation but also furthers knowledge on the optimal design of such feedback systems for experimentalists.

Natural cells exhibit rhythmic patterns of behavior, such as a beating heart, that help drive essential processes such as metabolism, signaling, growth, and division. To replicate these patterns in artificial cell compartments, scientists are exploring enzyme systems as key elements. Here, we report a more experimentally realistic numerical model of a system involving an encapsulated esterase enzyme that breaks down ethyl acetate to produce acid inside a compartment. We demonstrate how pH oscillations and bistability occur due to the coupling of the enzymatic production of acid and the transport of base through the compartment boundary and propose possible methods to enhance the likelihood of achieving sustained oscillations.

I. INTRODUCTION

Nonlinear responses and complex dynamic behavior in feedback systems are essential components of biological reaction networks. These feedback systems play a pivotal role in various regulatory mechanisms that allow living systems to maintain stability, control processes, and adapt to changing internal or environmental conditions. Oscillating chemical processes govern essential aspects of cell physiology, including circadian rhythms, DNA synthesis, glucose metabolism, cell division, hormone release, growth, and movement.[1–5] Without these biochemical fluctuations, cells would not be able to function. Research into the complexity of biologically relevant chemical reaction networks and strategies to enhance their ability to function across diverse parameter spaces has made significant strides.[6–17]

Biological cells are the fundamental unit of all living organisms. Replicating their inherent dynamic behavior and specific responses to stimuli in artificial cells is a significant challenge in synthetic biology, necessitating the development of minimal systems that mimic basic cellular functions. These developments will not only contribute to our basic understanding of cell function but also offer promising applications, such as the development of therapeutics that use biochemical oscillations for drug delivery with periodic release.[18]

Recent progress has yielded systems that emulate select cellular functions. Vesicles, polymersomes, and coacervates have acted as multi-compartment microreactors for cascade reactions that synthesize small organic molecules,[19,20] amplify DNA,[21–23] and display metabolism, growth, division, and motion.[22,24–26]

Enzymes, as powerful biological catalysts, accelerate chemical reactions with remarkable selectivity. Enzymes are sensitive to their environment and have specific ranges of activity, with pH being one of the most important factors influencing their functionality. The rate of an enzymatic process typically follows a bell-shaped pH curve, with the peak corresponding to a maximum activity at the pH at which the enzymes function most effectively. When an enzyme catalyzes a reaction that produces an acid or base, it exhibits auto-catalysis. The production of the product affects the pH, which brings it toward (positive feedback) or away from (negative feedback) the optimum pH of the enzyme, sparking interest in enzymatic pH oscillators. Enzyme-catalyzed reactions are a benign and biocompatible option for the generation of chemical feedback compared to traditional systems based on harsh redox chemistry.[27] Furthermore, oscillations driven by acid- or base-driven feedback could hold significance within biological systems, occurring with glycolysis, plant root growth, rhythmic production of cyclic AMP in slime moulds, and periodic muscle contractions in nemotodes.[3,28–34]

Fifty years ago, a feedback mechanism was proposed that used the bell-shaped rate–pH curve of enzymes and the formation of acidic or basic products.[35] This mechanism triggers an acceleration in the enzyme rate when the reaction generates non-neutral products and is initiated from a pH on the opposite side of the pH optimum. The concept was suggested to explain pH oscillations observed in their two-variable model involving an esterase enzyme called papain, which was attached to an artificial membrane. The pH oscillations were observed as a result of reaction and diffusion of a substrate (an ester) and hydrogen ions from the surrounding solution.

The concept of coupling an enzyme's bell-shaped pH–rate curve with transport mechanisms to induce dynamic behaviour should be applicable to a wide range of enzymes. Although numerous theoretical and numerical investigations have expanded the repertoire of autocatalytic enzymes and enzymatic oscillations driven by pH feedback, focusing on general systems,[36–38] or enzymes such as papain,[35,39–43] α-chymotrypsin[41] acetylcholinesterase,[40] protease,[40] and glucose oxidase,[44] experimental attempts to generate feedback by this mechanism have been sparse.[41,43,45–47] The scarcity may, in part, be attributed to ambiguities in kinetic enzyme data found in the literature, which are often measured at and, therefore, limited to very particular conditions.[48] Additionally, many studies on feedback in the original papain system have been hindered by simplified two-variable models that do not fully capture the complexities of acid and base transport. Specifically, these models assume equal rates of acid and base transport, which obscures the driving forces behind these oscillations.[35,40,42] These reaction–diffusion models took the diffusion of protons and, therefore, also hydroxide ions, as 15 times greater than the diffusion of the substrate. Bánsági and Taylor addressed this in the base-producing urea–urease system by building a three-variable model, allowing independent variation of the transport coefficients of substrate, acid and base.[49] This revealed a critical condition for oscillations in their

base-producing system: the transport of acid must exceed that of the substrate, urea. However, this constraint poses an experimental challenge because charged species are less permeable to biomembranes than neutral ones, and experimental observations confirming these conditions are yet to be reported.[49–52]

Advancements in synthetic biology have given us the capability to customize the characteristics of natural enzymes,[53] and researchers have successfully adjusted or reshaped the pH–rate curve of enzymes through various means. These include physical modifications such as immobilizing enzymes on an insoluble solid support,[54,55] chemical modifications using modifiers that interact with particular amino acids to alter the inherent properties of the enzyme,[56–58] and genetic engineering techniques such as modifying the sequence of amino acids or employing directed evolution to produce mutants with enhanced traits.[59–61] This presents opportunities for the deliberate design of enzymes with specific pH–rate curves, offering enhanced control over their potential dynamic behaviours.

The sensitivity of nonlinear enzyme systems has meant that any dynamic behavior that has been found has been shown to exist in a very small region of parameter space. To make these systems usable, this parameter space must be expanded. The current landscape lacks realistic models that encompass the complete experimentally feasible parameter space, a gap we aim to bridge. Esterases are a class of hydrolase enzymes that catalyze the hydrolysis of esters, converting them into acid and alcohol molecules. These enzymes function on a diverse range of substrates and play crucial roles in various biological functions. They have been isolated from a wide range of sources, including bacteria, fungi, algae, animals, plants, and humans, and function on several different substrates, highlighting their significance in numerous biochemical processes.[62] In this paper, we aim to use a more experimentally realistic and comprehensive model of an acid-producing esterase system and investigate the expansion of parameter space in which dynamic behavior could be found. By understanding the interplay between enzyme kinetics, acid–base reactions, and membrane dynamics, we can uncover novel insights into the generation and control of oscillatory behavior.

II. MODEL

The system was modelled as a set of coupled ordinary differential equations (ODEs) describing the rate of change of species in an esterase-loaded compartment. The esterase-catalyzed hydrolysis of ethyl acetate takes place via the following steps:
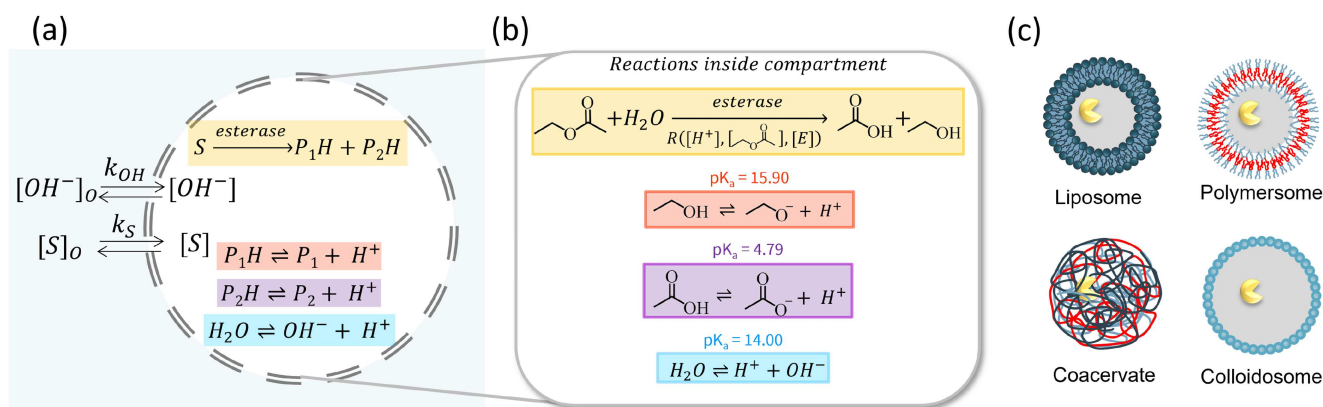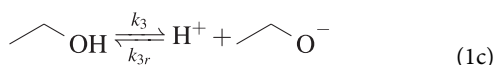

$$(1a)$$

$$(1b)$$
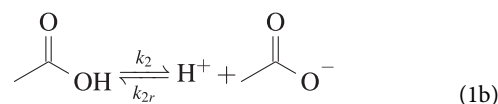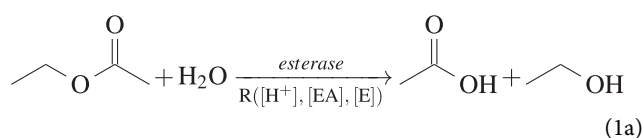
FIG. 1. (a) Reaction cell and overall key processes. The esterase enzyme catalyses the reaction of substrate (ethyl acetate) into products (acetic acid and ethanol) inside the compartment core. (b) Reactions that occur inside the compartment in the seven variable model of ethyl acetate hydrolysis: R, enzyme-catalysed rate; k_{OH}, exchange rate of base, OH^-; and k_S, exchange rate of substrate, ethyl acetate, with external solution of concentrations $[H^+]_0$ and $[ethyl\ acetate]_0$. (c) Examples of compartment structures that could house the enzyme reaction network.

$$ \diagdown\text{OH} \underset{k_{3r}}{\overset{k_3}{\rightleftharpoons}} \text{H}^+ + \diagdown\text{O}^- \tag{1c}$$

$$ \text{H}_2\text{O} \underset{k_{wr}}{\overset{k_w}{\rightleftharpoons}} \text{H}^+ + \text{OH}^- \tag{1d}$$

where the rate constants are $k_2 = 7.3 \times 10^5\,\text{s}^{-1}$, $k_{2r} = 4.5 \times 10^{10}\,\text{M}^{-1}\,\text{s}^{-1}$, $k_3 = 1.25 \times 10^{-6}\,\text{s}^{-1}$, $k_{3r} = 1 \times 10^{10}\,\text{M}^{-1}\,\text{s}^{-1}$, $k_w = 1 \times 10^{-4}\,\text{M}\,\text{s}^{-1}$, and $k_{wr} = 1 \times 10^{10}\,\text{M}^{-1}\,\text{s}^{-1}$ taken directly from the literature,[63] and R is as follows:

$$ R = \frac{V_{\max}[S]}{(K_M + [S])\left(1 + \frac{K_{es2}}{[H^+]} + \frac{[H^+]}{K_{es1}}\right)}. \tag{2}$$

S and H^+ denote substrate (ethyl acetate) and acid, respectively, while $V_{\max}$ is the maximum enzyme rate, equivalent to $k_{cat}[E]$, where k_{cat} is the turnover number, $[E]$ is the enzyme concentration, K_M is the Michaelis constant, K_{es1} and K_{es2} are the protonation equilibria of the substrate–enzyme complex that gives rise to the bell-shaped rate–pH curve. These enzyme-specific quantities have a range of values depending on the source of esterase (such as pig liver) and various conditions of the assays;[48] we explore variations in $V_{\max}$ here. The pH optimum of pig liver esterase has been quoted at $\sim$pH 7,[64–66] so we take values of the binding constants K_{es1} and K_{es2} to give that optimum. For simplicity, we write H^+ rather than H_3O^+. Given the high concentration of H_2O relative to other species, we can fix its concentration.

In the context of length scales considered, we assume a well-mixed compartment within a reservoir of outer solution. This requires the autocatalytic reaction time scale to be long compared to the diffusion time scale ($t = r^2/D$) in the compartment. Transport of species in and out of compartments with membranes, such as in liposomes, is typically characterized using permeability constants (P), while in those without membranes, such as in coacervates, would be described using diffusion constants (D). In this model, the

rate of change of the concentration of species is determined by the reaction rate and the net transfer rate between the compartment and the reservoir, where applicable,

$$ \frac{dA}{dt} = f(A) + k_A([A]_o - [A]), \tag{3}$$

where $f(A)$ contains all relevant reaction terms (including those of the enzyme, if applicable), k_A is the transport coefficient for the inflow of species A, $[A]$ is the concentration of species A, and $[A]_o$ is the constant concentration of species A in the reservoir. The transport coefficient can be related to diffusion or permeability coefficients by

$$ k_A \simeq \frac{D/\delta}{r} \tag{4}$$

and

$$ k_A \simeq \frac{3P}{r}, \tag{5}$$

where D is the diffusion coefficient, δ is the diffusion film of length, r is the radius of the compartment, and P is the permeability coefficient. While direct measurement of diffusion film thickness is often challenging,[67] permeability coefficients are shown to range from 10^{-3} to $10^{-8}\,\text{m s}^{-1}$,[68] depending on the thickness and properties of the bilayer and the properties of the species involved. Considering these permeability coefficients and a compartment radius of $10\,\mu\text{M}$, we obtain transport coefficient values that span from 10^{-3} to $10^2\,\text{s}^{-1}$.

The transport of OH^- in liposome-based systems may be limited due to the accumulation of charge or necessitate the flow of counterions to maintain electrochemical potential gradients.[69] Alternative structures such as colloidosomes or coacervates may offer more favorable conditions. In this study, the transfer rate of the base (k_{OH}) ranged between 0 and $0.055\,\text{s}^{-1}$, while that of the substrate (k_S) ranged from 0 to $0.022\,\text{s}^{-1}$. Dynamic behaviour was independent of k_H (as detailed in supplementary material S2).

A schematic representation of this model can be seen in Fig. 1. Numerical simulations of this seven-variable model were performed
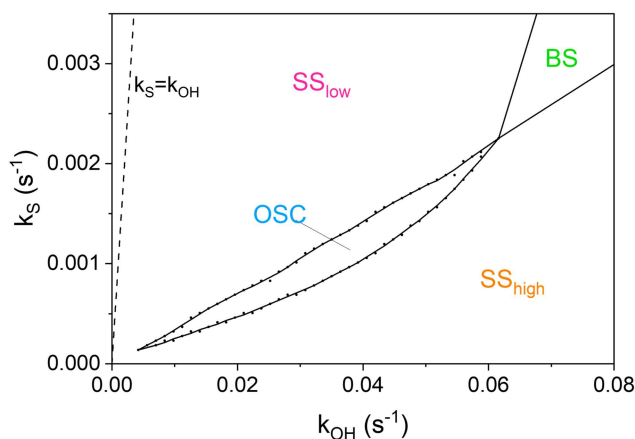
FIG. 2. Phase diagram in k_{OH}–k_S space with $[OH^-]_0 = 0.1$ mM, $[S]_0 = 3$ mM, $V_{max} = 1 \times 10^{-4}$ M s^{-1} ([E] = 0.5M assuming k_1 is 2×10^{-4} s^{-1}), where OSC, oscillatory; BS, bistable; SS$_{high}$, high pH steady state; and SS$_{low}$, low pH steady state. The dashed line marks $k_s = k_{OH}$.

using XPPAUT[70] with integration method CVODE. The XPPAUT file for this seven-variable model is given in supplementary material S1.

Our approach focuses on studying the range of parameters for oscillations using numerical simulations. Phase diagrams were created by incrementally increasing one parameter while keeping others constant (including the enzyme, substrate feed concentrations, and the hydroxide flow rate) and recording the pH data. A Python script was written to determine whether the pH value approached a steady state value or was oscillating, and this was manually confirmed for a subset of data using XPP.

III. RESULTS AND DISCUSSION

This system comprises positive feedback in the form of enzyme pH activity and negative feedback from base transport, k_{OH}. The ethyl acetate–esterase model, similar to the urea–urease model,[49] exhibits dynamic behavior within a specific parameter range. Figures 2 and 3(a) present phase diagrams in the k_{OH}–k_S and enzyme V_{max}–substrate concentration planes, respectively. These diagrams display parameter regions that give rise to singular steady states (low or high pH), bistability ("memory") where the pH reaches one of the two distinct states, or oscillations as parameters k_{OH} and k_S or V_{max} and $[S]_0$ are varied. Oscillations are observed when base transport is fast relative to the transport of substrates ($k_{OH} > k_S$), which allows the high steady state to recover as a result of the exchange of base and substrate with an external reservoir. As highlighted earlier, this aspect has been disregarded in prior analyses of esterase models that stipulate that proton transport must be faster than substrate transport, an assumption stemming from the equivalence of k_H and k_{OH} in oversimplified two-variable models.[40] This requirement for oscillations in the enzyme reactions may be contrasted from the other work in which fast autocatalyst diffusion and long-range activation led to oscillations.[71]
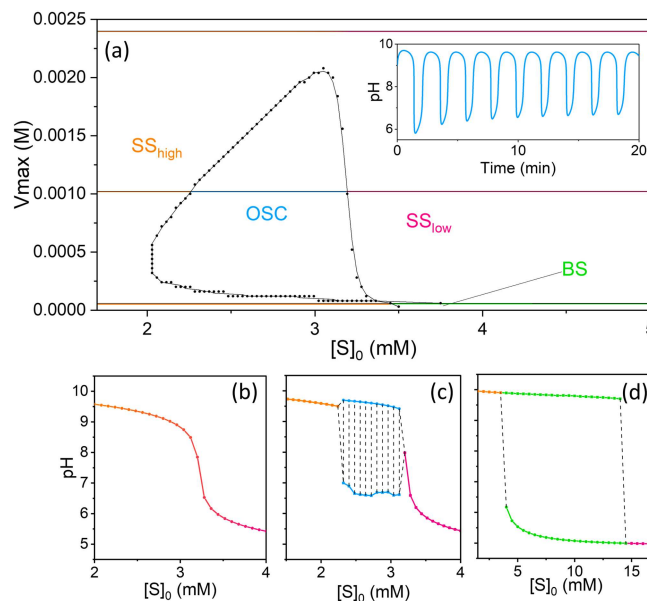

FIG. 3. (a) Phase diagram in $V_{max} - [S]_0$ space obtained with $[OH^-]_0 = 0.1$ mM, $k_{OH} = 0.045$ s^{-1}, and $k_S = 0.0014$ s^{-1}, where OSC, oscillatory region (blue); BS, bistable region (green); SS$_{high}$, high pH steady state region (orange); and SS$_{low}$, low pH steady state region (pink). Horizontal lines show the trajectories of the (b)–(d) bifurcation diagrams. The inset shows pH oscillations in time for $[S]_0 = 2.56$ mM and $V_{max} = 0.001\,02$ M s^{-1} ([E] = 12M assuming that k_1 is 2×10^{-4} s^{-1}). (b)–(d) pH–$[S]_0$ bifurcation diagrams obtained with $V_{max} =$ (b) 2.4×10^{-3} M s^{-1} ([E] = 5.1M assuming k_1 is 2×10^{-4} s^{-1}), (c) 1.02×10^{-3} M s^{-1} ([E] = 12 M assuming k_1 is 2×10^{-4} s^{-1}), and (d) 6×10^{-5} M s^{-1} ([E] = 0.3M assuming k_1 is 2×10^{-4} s^{-1}).

A typical pH-time trace for low steady state (pH clock), high steady state (no reaction), and an oscillation is shown in Fig. 4(a). Further insights from bifurcation diagrams, analyzed for three enzyme concentrations, reveal distinct responses. For higher enzyme concentrations, increasing substrate concentration leads to a rapid change in pH from high to low within a small substrate concentration range [Fig. 3(b)]. Intermediate enzyme concentrations trigger large oscillations between pH 6.6 and pH 9.6 across substrate concentrations of 2.32–3.12 mM [Fig. 3(c)]. Lower enzyme concentrations result in bistability between pH 6 and 9.7 over a wide range of substrate concentrations from 3.5 to 14.5 mM [Fig. 3(d)].

A. Oscillator characterization

The bifurcation diagrams presented here exhibit analogous traits to the urea–urease system.[49,51] In both cases, we observe a set of dynamics influenced by product activation through the enzyme pH–rate curve and negative feedback via transport. The two-variable model of the confined urea–urease reaction that displayed differential transport-driven oscillation was found to have canard-like behavior,[51] with the sudden appearance of large amplitude oscillations as a parameter is increased, and these shared traits would distinguish this enzyme/transport-driven system from some conventional feedback oscillators.[9,72]
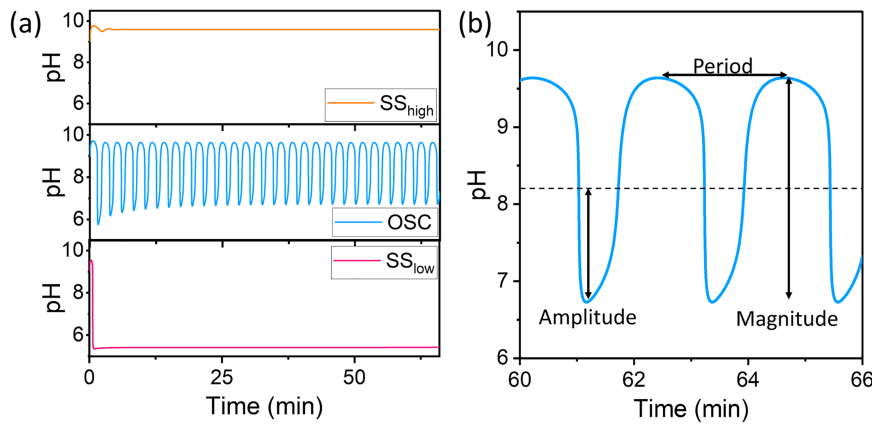
18 January 2024 13:56:47

FIG. 4. (a) pH-time traces obtained with $[OH^-]_0 = 0.1$ mM, $k_{OH} = 0.045$ s^{-1}, $k_S = 0.0014$ s^{-1}, and $V_{max} = 0.001\,02$ M s^{-1} ([E] = 12M assuming k_1 is 2×10^{-4} s^{-1}). The upper panel displays a high steady state at $[S]_0 = 4$ mM, the middle panel displays oscillations at $[S]_0 = 2.56$ mM, and lower panel displays a low steady state at $[S]_0 = 2$ mM. (b) Illustration depicting the definitions of period, magnitude, and amplitude of an oscillation.

Figure 5 illustrates the amplitude and frequency characteristics of the oscillations within the $V_{max} - [S]_0$ parameter space of $k_{OH} = 0.055$ s^{-1}. Sets of points correspond to different $[S]_0$ values, connected by lines denoting shared V_{max} values. We observe a small range of frequencies and amplitudes over which the oscillator functioned (30- and 11-fold increase, respectively), in contrast to activator–inhibitor systems that display flexible frequency tuning alongside relatively constant amplitudes.[73] Figure 5(b) displays examples of pH–time oscillations for three V_{max} values. This oscillator achieves similar stability in oscillation frequency to temperature-compensated oscillators;[74] however, its stability is maintained across a range of controllable experimental parameters. The shape of the amplitude/frequency curves seems to suggest the simultaneous acceleration of positive and negative feedback mechanisms as we navigate parameter space; however, there appears to be a bounded region of accessible frequencies. For many applications, robust oscillations in both amplitude and frequency may be required. Such requirements emerge in scenarios that demand reliability of response or precise timing for processes such as neural networks,[2] circadian rhythms,[75] or genetic oscillators within embryonic development.[76]

B. Tunability of the system

The ethyl acetate–esterase model exhibits oscillations across a broader range of enzyme ([E]) and substrate ($[S]_0$) concentrations compared to the urea–urease model,[49] suggesting its suitability as an experimentally observable oscillatory system when the condition $k_{OH} > k_S$ is met. This observation naturally leads us to investigate the broader tunability of the system through experimentally controllable parameters.

The size of the parameter space in which sustained oscillations can be found expands as k_{OH}/k_S ratios increase (Fig. 6). For instance, when the k_{OH}/k_S ratio exceeds 10.7 ($k_S = 0.0014$ s^{-1}, $k_{OH} = 0.015$ s^{-1}), a practically feasible concentration range for both substrate and enzyme exists, which enhances the prospects of experimentalists' encountering oscillations. Specifically, oscillations can be observed within the substrate concentration range of 0.8 to 1.04 mM and enzyme concentrations spanning from 0.6 to 3.6 mM (assuming k_1 is 2×10^{-4} s^{-1} as $V_{max} = 1.2 \times 10^{-4}$–$4.2 \times 10^{-4}$ M s^{-1}). With experimentally determined diffusion coefficients in water of $D_{OH} = 5.3 \times 10^{-5}$ cm^2 s^{-1} and $D_S = 1 \times 10^{-5}$ cm^2 s^{-1}, the ratio of D_{OH}/D_S is 5.3.[77,78]
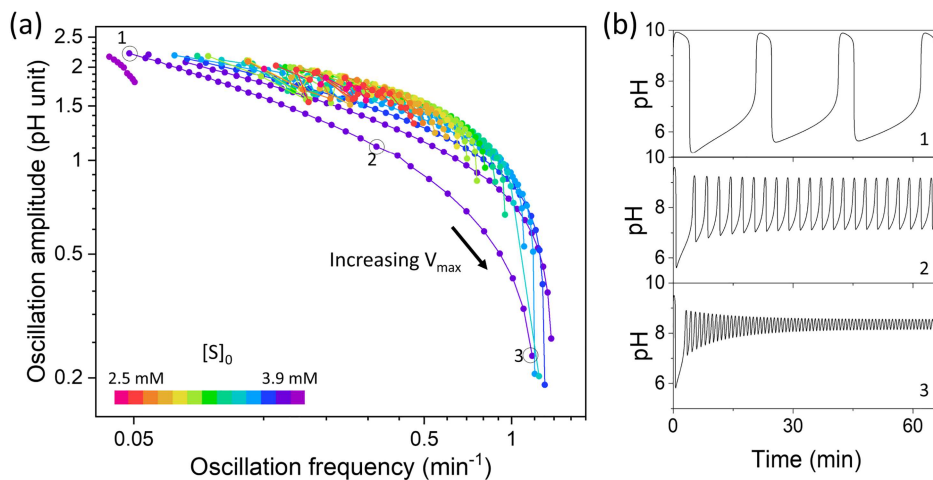
FIG. 5. (a) Amplitude/frequency curves for the oscillations in V_{max} vs $[S]_0$ parameter space for $k_{OH} = 0.055$ s^{-1}. Line colors represent different $[S]_0$ values. Lines connect points with the same $[S]_0$, revealing amplitude/frequency trends with varying V_{max} and demonstrating how experimentally accessible adjustments in V_{max} and $[S]_0$ influence oscillation amplitude and frequency within the defined parameter space. (b) pH-time traces depict oscillation variations at three V_{max} values along the $[S]_0 = 3.8$ mM line corresponding to positions 1, 2, and 3 in (a). These V_{max} values are 1.8×10^{-4}, 1.44×10^{-4}, and 2.04×10^{-4} M s^{-1}, respectively.

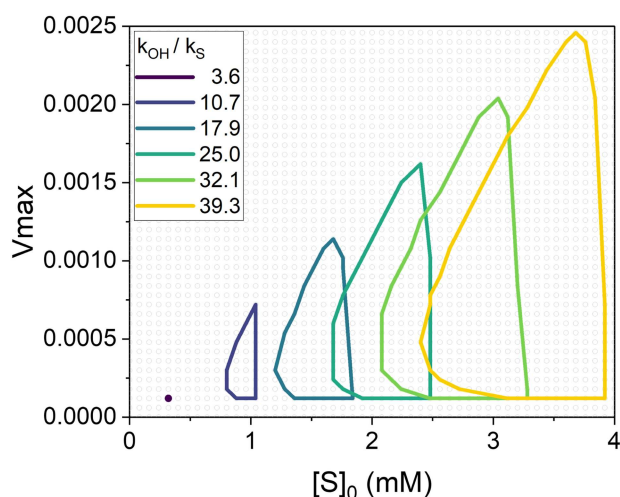**FIG. 6.** Phase plots at various k_{OH} values as a function of the parameters $[S]_0$ and V_{max} obtained with $[OH^-]_0 = 0.1$ mM and $k_S = 0.0014$ s^{-1}. Larger values of k_{OH} lead to larger regions of $V_{max} - [S]_0$-space in which sustained oscillations are observed.

Several strategies exist to potentially enhance this D_{OH}/D_S ratio. Diffusion and permeability have been shown to decrease when the chain length of the organic molecule is extended,[79] modifying the composition of the diffusing solution, such as adding 30% sucrose,[80] immobilizing the substrate on large molecules such as starch,[81,82] and fine-tuning the compartment formulations of coacervates or polymersomes.[83] Implementing any of these methods could yield diffusion ratios that align well with the transport rate ratios for oscillations shown in Figs. 2 and 6 and the values of 32 and 39 in Figs. 3–5 and Fig. 7. However, achieving the condition of rapid OH$^-$ transport in liposome-based systems may prove challenging due to the requirement to maintain the electrochemical potential gradient across the bilayer.[69] Alternative constructs like colloidosomes

or coacervates may prove more favorable for achieving the desired diffusion ratios.

The positioning of the pH–rate curve of the esterase enzyme has a notable impact on the occurrence of sustained oscillations within the $V_{max} - [S]_0$ parameter space, as illustrated in Fig. 7. A pH–rate curve with an optimum at pH 6 expands the oscillatory region in the V_{max} and $[S]_0$ space. Conversely, a pH optimum of 8 diminishes the oscillatory region. The critical factor is the location of the right side of the bell-shape in this curve (supplementary material S3). Figure 7(c) shows that each unit of decrease in the optimum pH increases the V_{max} space where oscillations can be detected by a factor of 10. This highlights the importance of positioning the enzyme's pH optimum to facilitate rate acceleration at lower pH levels to improve experimental feasibility and maximize the chances of finding oscillations in this system.

The potential tunability shown here highlights the intricacies involved in the interplay between transport pheomena and enzyme kinetics and offers insights into optimizing conditions for various biochemical processes.

IV. CONCLUSIONS

In summary, this study presents a seven-variable kinetic model for an esterase-based system that produces acid. The aim is to make it easier to experimentally investigate how interactions between the enzyme's pH–rate curve and transport-mediated negative feedback create dynamic behaviors. We identify ranges of parameters that can be controlled in experiments, leading to two interesting phenomena: bistability and sustained pH oscillations. Our numerical results not only identify the conditions necessary for these oscillations but also provide suggestions for expanding the range of parameters that support such behaviors. This includes adjusting the enzyme's pH–rate curve and recognizing the role of negative feedback. These findings provide valuable insights into how numerous variables within the reaction pathway interact in driving dynamic behaviour. Moreover, they offer guidance for designing chemical oscillators based on similar principles. With further investigation into tuning the reaction network to make dynamic behavior more
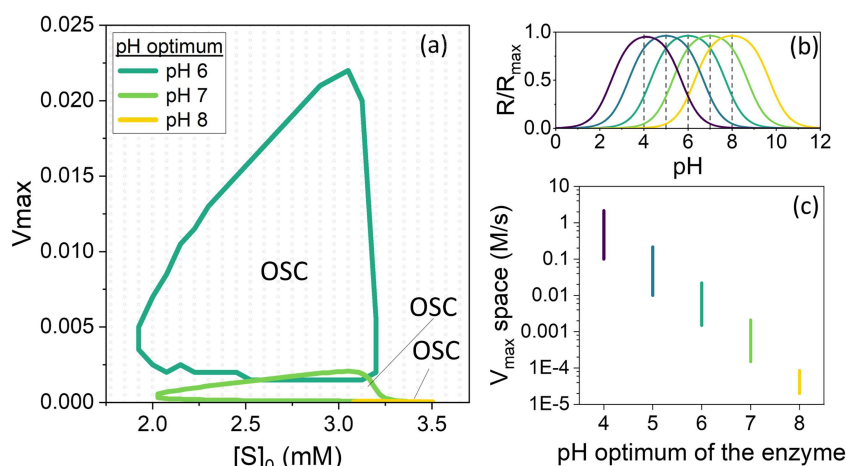
FIG. 7. (a) Impact of varying the enzyme's pH optimum on the region of $V_{max} - [S]_0$ space in which sustained oscillations are observed. The color-coded regions distinguish oscillatory zones for enzyme pH-rate maxima at pH 6 (dark green), 7 (light green), and 8 (yellow). Parameters: $[OH^-]_0 = 0.1$ mM, $k_{OH} = 0.045$ s^{-1}, and $k_S = 0.0014$ s^{-1}. (b) Corresponding normalized pH-rate curves of the enzyme. (c) Maximum range of V_{max} values that give rise to oscillations as a function enzyme optimum pH, ranging from pH 4 to pH 8, displayed on a logarithmic scale.

accessible and with more reliable literature and kinetic data, especially for non-neutral pH conditions where these enzyme systems operate, achieving experimental oscillations in this system becomes increasingly promising.

SUPPLEMENTARY MATERIAL

The supplementary information provides the XPP model code (S1), an exploration of the impact of proton transport (Fig. S2), additional analysis of the affect of the enzyme's pH–rate curve on oscillations (Fig. S3), and an extension of the information presented in Fig. 5 (Fig. S4).

ACKNOWLEDGMENTS

AUTHOR DECLARATIONS

Conflict of Interest

The authors have no conflicts to disclose.

Author Contributions

Anna S. Leathard: Investigation (lead); Methodology (equal); Writing – original draft (lead); Writing – review & editing (equal). **Paul A. Beales:** Conceptualization (equal); Funding acquisition (lead); Writing – review & editing (equal). **Annette F. Taylor:** Conceptualization (equal); Methodology (equal); Supervision (lead); Writing – review & editing (equal).

DATA AVAILABILITY

The data that support the findings of this study are available from the corresponding author upon reasonable request.

REFERENCES

[1]I. R. Epstein, K. Kustin, P. De Kepper, and M. Orbán, "Oscillating chemical reactions," Sci. Am. **248**, 112–123 (1983).
[2]R. R. Llinás, A. A. Grace, and Y. Yarom, "In vitro neurons in mammalian cortical layer 4 exhibit intrinsic oscillatory activity in the 10- to 50-Hz frequency range," Proc. Natl. Acad. Sci. U.S.A. **88**, 897–901 (1991).
[3]H. F. Chou, N. Berman, and E. Ipp, "Oscillations of lactate released from islets of langerhans: Evidence for oscillatory glycolysis in beta-cells," Am. J. Physiol.-Endocrinol. Metab. **262**, E800–E805 (1992).
[4]A. Goldbeter, "Oscillatory enzyme reactions and Michaelis-Menten kinetics," FEBS Lett. **587**, 2778–2784 (2013).
[5]Y. Miele, Z. Medveczky, G. Holló, B. Tegze, I. Derényi, Z. Hórvölgyi, E. Altamura, I. Lagzi, and F. Rossi, "Self-division of giant vesicles driven by an internal enzymatic reaction," Chem. Sci. **11**, 3228–3235 (2020).
[6]A. Goldbeter and O. Decroly, "Temporal self-organization in biochemical systems: Periodic behavior vs chaos," Am. J. Physiol.-Regul. Integr. Comp. Physiol. **245**, R478–R483 (1983).
[7]I. R. Epstein and K. Showalter, "Nonlinear chemical dynamics: Oscillations, patterns, and chaos," J. Phys. Chem. **100**, 13132–13147 (1996).
[8]Z. Dadon, N. Wagner, and G. Ashkenasy, "The road to non-enzymatic molecular networks," Angew. Chem., Int. Ed. **47**, 6128–6136 (2008).
[9]B. Novák and J. J. Tyson, "Design principles of biochemical oscillators," Nat. Rev. Mol. Cell. Biol. **9**, 981–991 (2008).
[10]N. Wagner, S. Alasibi, E. Peacock-Lopez, and G. Ashkenasy, "Coupled oscillations and circadian rhythms in molecular replication networks," J. Phys. Chem. Lett. **6**, 60–65 (2014).
[11]S. N. Semenov, A. S. Wong, R. M. van der Made, S. G. Postma, J. Groen, H. W. van Roekel, T. F. de Greef, and W. T. Huck, "Rational design of functional and tunable oscillating enzymatic networks," Nat. Chem. **7**, 160–165 (2015).
[12]S. N. Semenov, L. J. Kraft, A. Ainla, M. Zhao, M. Baghbanzadeh, V. E. Campbell, K. Kang, J. M. Fox, and G. M. Whitesides, "Autocatalytic, bistable, oscillatory networks of biologically relevant organic reactions," Nature **537**, 656–660 (2016).
[13]A. S. Wong, A. A. Pogodaev, I. N. Vialshin, B. Helwig, and W. T. Huck, "Molecular engineering of robustness and resilience in enzymatic reaction networks," J. Am. Chem. Soc. **139**, 8146–8151 (2017).
[14]N. Wagner, D. Hochberg, E. Peacock-Lopez, I. Maity, and G. Ashkenasy, "Open prebiotic environments drive emergent phenomena and complex behavior," Life **9**, 45 (2019).
[15]B. J. Cafferty, A. S. Wong, S. N. Semenov, L. Belding, S. Gmür, W. T. Huck, and G. M. Whitesides, "Robustness, entrainment, and hybridization in dissipative molecular networks, and the origin of life," J. Am. Chem. Soc. **141**, 8289–8295 (2019).
[16]B. Dúzs, I. Lagzi, and I. Szalai, "Functional rhythmic chemical systems governed by pH-driven kinetic feedback," ChemSystemsChem **5**, e202300004 (2023).
[17]E. Lantos, G. Mótyán, É. Frank, R. Eelkema, J. van Esch, D. Horváth, and Á. Tóth, "Dynamics of hydroxide-ion-driven reversible autocatalytic networks," RSC Adv. **13**, 20243–20247 (2023).
[18]S. J. Jones, A. F. Taylor, and P. A. Beales, "Towards feedback-controlled nanomedicines for smart, adaptive delivery," Exp. Biol. Med. **244**, 283–293 (2018).
[19]Y. Elani, R. V. Law, and O. Ces, "Vesicle-based artificial cells as chemical microreactors with spatially segregated reaction pathways," Nat. Commun. **5**, 5305 (2014).
[20]R. J. Peters, M. Marguet, S. Marais, M. W. Fraaije, J. C. van Hest, and S. Lecommandoux, "Cascade reactions in multicompartmentalized polymersomes," Angew. Chem. **126**, 150–154 (2013).
[21]S. Lee, H. Koo, J. H. Na, K. E. Lee, S. Y. Jeong, K. Choi, S. H. Kim, I. C. Kwon, and K. Kim, "Dna amplification in neutral liposomes for safe and efficient gene delivery," ACS Nano **8**, 4257–4267 (2014).
[22]K. Kurihara, M. Tamura, K. Shohda, T. Toyota, K. Suzuki, and T. Sugawara, "Self-reproduction of supramolecular giant vesicles combined with the amplification of encapsulated dna," Nat. Chem. **3**, 775–781 (2011).
[23]T. Oberholzer, M. Albrizio, and P. L. Luisi, "Polymerase chain reaction in liposomes," Chem. Biol. **2**, 677–682 (1995).
[24]H.-J. Choi and C. D. Montemagno, "Artificial organelle: ATP synthesis from cellular mimetic polymersomes," Nano Lett. **5**, 2538–2542 (2005).
[25]K. K. Nakashima, M. H. van Haren, A. A. André, I. Robu, and E. Spruijt, "Active coacervate droplets are protocells that grow and resist ostwald ripening," Nat. Commun. **12**, 3819 (2021).
[26]A. C. Hortelão, S. García-Jimeno, M. Cano-Sarabia, T. Patiño, D. Maspoch, and S. Sanchez, "Lipobots: Using liposomal vesicles as protective shell of urease-based nanomotors," Adv. Funct. Mater. **30**, 2002767 (2020).
[27]I. R. Epstein and J. A. Pojman, *An Introduction to Nonlinear Chemical Dynamics: Oscillations, Waves, Patterns, and Chaos* (Oxford University Press, 1998).
[28]M. J. Hauser, "Synchronisation of glycolytic activity in yeast cells," Curr. Genet. **68**, 69–81 (2021).
[29]S. Mangano, J. M. Pacheco, C. Marino-Buslje, and J. M. Estevez, "How does ph fit in with oscillating polar growth?," Trends Plant Sci. **23**, 479–489 (2018).
[30]A. Lovy-Wheeler, J. G. Kunkel, E. G. Allwood, P. J. Hussey, and P. K. Hepler, "Oscillatory increases in alkalinity anticipate growth and may regulate actin dynamics in pollen tubes of lily," Plant Cell **18**, 2182–2193 (2006).
[31]K. Gottmann and C. J. Weijer, "In situ measurements of external ph and optical density oscillations in dictyostelium discoideum aggregates," J. Cell Biol. **102**, 1623–1629 (1986).
[32]D. Malchow, V. Nanjundiah, and G. Gerisch, "pH oscillations in cell suspensions of dictyostelium discoideum: Their relation to cyclic-amp signals," J. Cell Sci. **30**, 319–330 (1978).
[33]B. J. Dodd and J. M. Kralj, "Live cell imaging reveals ph oscillations in saccharomyces cerevisiae during metabolic transitions," Sci. Rep. **7**, 13922 (2017).

18 January 2024 13:56:47

[34]A. A. Beg, G. G. Ernstrom, P. Nix, M. W. Davis, and E. M. Jorgensen, "Protons act as a transmitter for muscle contraction in C. elegans," Cell **132**, 149–160 (2008).

[35]S. R. Caplan, A. Naparstek, and N. J. Zabusky, "Chemical oscillations in a membrane," Nature **245**, 364–366 (1973).

[36]H.-S. Hahn, A. Nitzan, P. Ortoleva, and J. Ross, "Threshold excitations, relaxation oscillations, and effect of noise in an enzyme reaction," Proc. Natl. Acad. Sci. U.S.A. **71**, 4067–4071 (1974).

[37]N. J. Zabusky and R. H. Hardin, "Phase transition, stability, and oscillations for an autocatalytic, single, first-order reaction in a membrane," Phys. Rev. Lett. **31**, 812–815 (1973).

[38]T. R. Chay, "A model for biological oscillations," Proc. Natl. Acad. Sci. U.S.A. **78**, 2204–2207 (1981).

[39]A. Goldbeter and S. R. Caplan, "Oscillatory enzymes," Annu. Rev. Biophys. Bioeng. **5**, 449–476 (1976).

[40]P. Shen and R. Larter, "Role of substrate inhibition kinetics in enzymatic chemical oscillations," Biophys. J. **67**, 1414–1428 (1994).

[41]T. Ohmori, M. Nakaiwa, T. Yamaguchi, M. Kawamura, and R. Y. Yang, "Self-sustained ph oscillations in a compartmentalized enzyme reactor system," Biophys. Chem. **67**, 51–57 (1997).

[42]J. Zagora, M. Voslař, L. Schreiberová, and I. Schreiber, "Excitability in chemical and biochemical pH-autocatalytic systems," Faraday Discuss. **120**, 313–324 (2001).

[43]A. Naparstek, D. Thomas, and S. Roy Caplan, "An experimental enzyme-membrane oscillator," Biochim. Biophys. Acta (BBA)—Biomembranes **323**, 643–646 (1973).

[44]V. K. Vanag, D. G. Míguez, and I. R. Epstein, "Designing an enzymatic oscillator: Bistability and feedback controlled oscillations with glucose oxidase in a continuous flow stirred tank reactor," J. Chem. Phys. **125**, 194515 (2006).

[45]J. Temminck Groll, "Periodische erscheinungen bei fermenten als folge ihrer kolloiden beschaffenheit," Kolloid-Zeitschrift **21**, 138–148 (1917).

[46]A. Friboulet and D. Thomas, "Electrical excitability of artificial enzyme membranes," Biophys. Chem. **16**, 153–157 (1982).

[47]G. Bodó, R. M. Branca, Á. Tóth, D. Horváth, and C. Bagyinka, "Concentration-dependent front velocity of the autocatalytic hydrogenase reaction," Biophys. J. **96**, 4976–4983 (2009).

[48]A. G. McDonald and K. F. Tipton, "Parameter reliability and understanding enzyme function," Molecules **27**, 263 (2022).

[49]T. Bánsági and A. F. Taylor, "Role of differential transport in an oscillatory enzyme reaction," J. Phys. Chem. B **118**, 6092–6097 (2014).

[50]Y. Miele, T. Bánsági, A. F. Taylor, and F. Rossi, "Modelling approach to enzymatic ph oscillators in giant lipid vesicles," in Advances in Bionanomaterials. Lecture Notes in Bioengineering, edited by S. Piotto, F. Rossi, S. Concilio, E. Reverchon, and G. Cattaneo (Springer, Cham, 2017).

[51]A. V. Straube, S. Winkelmann, C. Schütte, and F. Höfling, "Stochastic ph oscillations in a model of the urea–urease reaction confined to lipid vesicles," J. Phys. Chem. Lett. **12**, 9888–9893 (2021).

[52]Y. Miele, S. J. Jones, F. Rossi, P. A. Beales, and A. F. Taylor, "Collective behavior of urease ph clocks in nano- and microvesicles controlled by fast ammonia transport," J. Phys. Chem. Lett. **13**, 1979–1984 (2022).

[53]P. Villeneuve, J. M. Muderhwa, J. Graille, and M. J. Haas, "Customizing lipases for biocatalysis: A survey of chemical, physical and molecular biological approaches," J. Mol. Catal. B: Enzym. **9**, 113–148 (2000).

[54]N. Tüzmen, T. Kalburcu, and A. Denizli, "α-amylase immobilization onto dye attached magnetic beads: Optimization and characterization," J. Mol. Catal. B: Enzym. **78**, 16–23 (2012).

[55]M. I. Kim, H. O. Ham, S.-D. Oh, H. G. Park, H. N. Chang, and S.-H. Choi, "Immobilization of mucor javanicus lipase on effectively functionalized silica nanoparticles," J. Mol. Catal. B: Enzym. **39**, 62–68 (2006).

[56]S. Saraswathi and M. Keyes, "Semisynthetic 'acid-esterase': Conformational modification of ribonuclease," Enzyme Microb. Technol. **6**, 98–100 (1984).

[57]G. DeSantis and J. B. Jones, "Chemical modifications at a single site can induce significant shifts in the pH profiles of a serine protease," J. Am. Chem. Soc. **120**, 8582–8586 (1998).

[58]X. Liang, W. Zhang, J. Ran, J. Sun, L. Jiao, L. Feng, and B. Liu, "Chemical modification of sweet potato β-amylase by mal-mpeg to improve its enzymatic characteristics," Molecules **23**, 2754 (2018).

[59]X. Chu, H. He, C. Guo, and B. Sun, "Identification of two novel esterases from a marine metagenomic library derived from South China Sea," Appl. Microbiol. Biotechnol. **80**, 615–625 (2008).

[60]M. L. Ludwiczek, I. D'Angelo, G. N. Yalloway, J. A. Brockerman, M. Okon, J. E. Nielsen, N. C. Strynadka, S. G. Withers, and L. P. McIntosh, "Strategies for modulating the pH-dependent activity of a family 11 glycoside hydrolase," Biochemistry **52**, 3138–3156 (2013).

[61]S. Pokhrel, J. C. Joo, Y. H. Kim, and Y. J. Yoo, "Rational design of a bacillus circulans xylanase by introducing charged residue to shift the ph optimum," Process Biochem. **47**, 2487–2493 (2012).

[62]S. Sood, A. Sharma, N. Sharma, and S. S. Kanwar, "Carboxylesterases: Sources, characterization and broader applications," Insights Enzym. Res. **01**, 1–11 (2018).

[63]M. Eigen, "Proton transfer, acid-base catalysis, and enzymatic hydrolysis. part I: Elementary processes," Angew. Chem., Int. Ed. Engl. **3**, 1–19 (1964).

[64]W. Junge and E. Heymann, "Characterization of the isoenzymes of pig-liver esterase 2. kinetic studies," Eur. J. Biochem. **95**, 519–525 (1979).

[65]K.-M. Park, J.-H. Lee, S.-C. Hong, C. W. Kwon, M. Jo, S. J. Choi, K. Kim, and P.-S. Chang, "Selective production of 1-monocaprin by porcine liver carboxylesterase-catalyzed esterification: Its enzyme kinetics and catalytic performance," Enzyme Microb. Technol. **82**, 51–57 (2016).

[66]H. A. Sousa, C. A. Afonso, and J. G. Crespo, "Kinetic study of the enantioselective hydrolysis of a meso-diester using pig liver esterase," J. Chem. Technol. Biotechnol. **75**, 707–714 (2000).

[67]B. G. Cox, Modern Liquid Phase Kinetics (Oxford University Press, 1994).

[68]A. Walter and J. Gutknecht, "Permeability of small nonelectrolytes through lipid bilayer membranes," J. Membr. Biol. **90**, 207–217 (1986).

[69]M. Megens, C. E. Korman, C. M. Ajo-Franklin, and D. A. Horsley, "Faster-than-anticipated Na+/Cl- diffusion across lipid bilayers in vesicles," Biochim. Biophys. Acta (BBA)—Biomembr. **1838**, 2420–2424 (2014).

[70]B. Ermentrout, "Simulating, analyzing, and animating dynamical systems: A guide to xppaut for researchers and students," Appl. Mech. Rev. **56**, B53 (2003).

[71]M. Fuentes, M. N. Kuperman, J. Boissonade, E. Dulos, F. Gauffre, and P. De Kepper, "Dynamical effects induced by long range activation in a nonequilibrium reaction-diffusion system," Phys. Rev. E **66**, 056205 (2002).

[72]M. Orbán, K. Kurin-Csörgei, and I. R. Epstein, "pH-regulated chemical oscillators," Acc. Chem. Res. **48**, 593–601 (2015).

[73]T. Y.-C. Tsai, Y. S. Choi, W. Ma, J. R. Pomerening, C. Tang, and J. E. Ferrell, "Robust, tunable biological oscillations from interlinked positive and negative feedback loops," Science **321**, 126–129 (2008).

[74]S. Chakravarty, C. Hong, and A. Csikász-Nagy, "A. systematic analysis of negative and positive feedback loops for robustness and temperature compensation in circadian rhythms," npj Syst. Biol. Appl. **9**, 126–129 (2023).

[75]J. Bass, "Circadian topology of metabolism," Nature **491**, 348–356 (2012).

[76]K. Uriu, "Genetic oscillators in development," Dev. Growth Differ. **58**, 16–30 (2016).

[77]E. L. Cussler, Diffusion: Mass Transfer in Fluid Systems (Cambridge University Press, 2009).

[78]P. Vanysek, "Conductivity ionic diffusion at infinite dilution," in CRC Handbook of Chemistry and Physics, 92nd ed., edited by W. M. Haynes and D. R. Lide (CRC Press/Taylor and Francis Group, Boca Raton, FL, 2011), pp. 77–79.

[79]P. Rogers and W. McElroy, "Enzymic determination of aldehyde permeability in luminous bacteria. I. effect of chain length on light emission and penetration," Arch. Biochem. Biophys. **75**, 87–105 (1958).

[80]D. D. Frey and C. J. King, "Diffusion coefficients of acetates in aqueous sucrose solutions," J. Chem. Eng. Data **27**, 419–422 (1982).

[81]I. Lengyel and I. R. Epstein, "A chemical approach to designing Turing patterns in reaction-diffusion systems," Proc. Natl. Acad. Sci. U.S.A. **89**, 3977–3979 (1992).

[82]J. Horváth, I. Szalai, and P. De Kepper, "An experimental design method leading to chemical turing patterns," Science **324**, 772–775 (2009).

[83]A. J. Miller, A. K. Pearce, J. C. Foster, and R. K. O'Reilly, "Probing and tuning the permeability of polymersomes," ACS Cent. Sci. **7**, 30–38 (2020).

18 January 2024 13:56:47